Ionization-induced blueshift of high-peak-power guided-wave ultrashort laser pulses in hollow-core photonic-crystal fibers

A. B. Fedotov, E. E. Serebryannikov, and A. M. Zheltikov*
Physics Department, International Laser Center, M. V. Lomonosov Moscow State University, Vorob'evy gory, Moscow 119992, Russia
(Received 20 March 2007; revised manuscript received 2 July 2007; published 8 November 2007)

Ionization-induced change in the refractive index of a gas is shown to give rise to a substantial spectral blueshift of megawatt light pulses transmitted through a gas-filled hollow photonic-crystal fiber (PCF). This effect suggests the ways of controlling not only the rate, but also the sign of the soliton frequency shift for high-peak-power ultrashort light pulses guided in hollow PCFs filled with Raman-active ionizing gases.

DOI: 10.1103/PhysRevA.76.053811 PACS number(s): 42.65.Wi, 42.81.Qb

Short laser pulses propagating in media with retarded optical nonlinearity undergo a continuous frequency downshift, a phenomenon which is readily understood in the spectral domain as the Raman amplification of the long-wavelength part of the spectrum leading to the depletion of its short-wavelength wing. In the regime of anomalous dispersion in optical fibers, this effect manifests itself as a soliton-self-frequency shift (SSFS) [1], pushing solitons toward longer wavelengths. Highly nonlinear photonic-crystal fibers (PCFs) [2,3] can radically enhance the SSFS [4], allowing the creation of compact and efficient fiber-format frequency-tunable sources [5,6]. In these fibers, the key SSFS parameters, such as the frequency-shift rate and the energy carried by redshifting solitons, can be controlled through fiber design. The sign of the frequency shift, however, remains beyond control, as the redshifting is inherent in the nature of the Raman-type optical nonlinearity. Here we show, both experimentally and theoretically, that, through ionization-induced optical nonlinearity in hollow-core PCFs, guided-wave short-pulse laser fields can be forced to do what they strongly resist—they can be spectrally shifted toward higher frequencies.

We start with qualitative arguments explaining the basic physical phenomena leading to a blueshift of high-peak-power ultrashort laser pulses in gas media. With an intensity of a laser pulse being high enough to ionize the gas, free electrons generated as a result of this ionization process reduce the refractive index of the gas medium at the frequency ω_0 by [7] $\delta n_p(t) \approx -[\omega_p(t)]^2/(2\omega_0^2)$, where $\omega_p(t) = [4\pi e^2 n_e(t)/m_e]^{1/2}$ is the plasma frequency, e and m_e are the electron charge and mass, respectively, and $n_e(t)$ is the density of free electrons produced by the laser pulse. Since the time-dependent electron density $n_e(t)$ monotonically increases as long as the short-pulse laser field is on, $\delta n_p(t)$ is also a monotonic function of time, leading to a monotonic decrease in the refractive index of the gas in the course of the laser pulse and inducing a phase shift of the laser pulse $\varphi_p(t) = \omega_0 l \delta n_p(t)/c$, where l is the length of the ionizing gas medium and c is the speed of light. The time-dependent phase shift gives rise to a frequency shift of the laser pulse, $\delta\omega_p \approx -\partial\varphi_p(t)/\partial t = -(\omega_0 l/c)\partial[\delta n_p(t)]/\partial t$. As the electron density $n_e(t)$ persistently increases as long as the short-pulse laser field is on, $\partial[\delta n_p(t)]/\partial t < 0$ not only in the leading edge, but within the entire laser pulse (inset 1 in Fig. 1). Thus the ionization-induced time-dependent change in the refractive index of a gas medium translates into a blueshift of the laser pulse, $\delta\omega_p > 0$.

The above-outlined simple scenario of blueshifting has been identified in earlier work [7] on the dynamics and spectral transformations of high-intensity laser pulses in ionizing gas media. We now show that, in the waveguide regime, this effect may lead to interesting and significant consequences, competing with a redshift of optical solitons induced by the Raman effect and giving rise to a net blueshifting of high-peak-power solitonic features of the laser field. To demonstrate these effects, we model the propagation dynamics of a high-peak-power ultrashort laser pulse in a gas-filled hollow-core PCF using the pulse-evolution equation [8–10] for the field envelope $A(z,\tau)$ including the gas and waveguide dispersion, ionization-induced loss, Kerr and Raman nonlinearities of the gas, the shock-wave term, and ionization-induced change in the refractive index:

$$\begin{aligned}\frac{\partial A(z,\tau)}{\partial z} = &-\frac{1}{2}\left[\alpha + \frac{I_p}{I(z,\tau)}\frac{\partial n_e(z,\tau)}{\partial \tau}\right]A(z,\tau) \\ &- \sum_{m=2}^{6}\frac{i^{m+1}}{m!}\beta_m\frac{\partial^m A}{\partial \tau^m} + i\gamma_{core}\left(1+\frac{i}{\omega_0}\frac{\partial}{\partial\tau}\right)A(z,\tau) \\ &\times\int_{-\infty}^{\tau} R_{core}(\theta)|A(z,\tau-\theta)|^2 d\theta \\ &+ i\gamma_{cl}\left(1+\frac{i}{\omega_0}\frac{\partial}{\partial\tau}\right)A(z,\tau) \\ &\times\int_{-\infty}^{\tau} R_{cl}(\theta)|A(z,\tau-\theta)|^2 d\theta \\ &- ik_0\frac{[\omega_p(z,\tau)]^2}{2\omega_0^2}A(z,\tau-\theta), \end{aligned} \tag{1}$$

where α is the attenuation coefficient, which includes the waveguide loss, $\tau = t - z/u$, u is the group velocity at the central frequency of the input pump field, $I(z,\tau)$ is the field intensity, I_p is the ionization potential, n_e is the electron density, $\beta_m = (\partial^m\beta/\partial\omega^m)_{\omega=\omega_0}$, β is the propagation constant of the waveguide mode, ω_0 is the central frequency of the laser

*zheltikov@phys.msu.ru

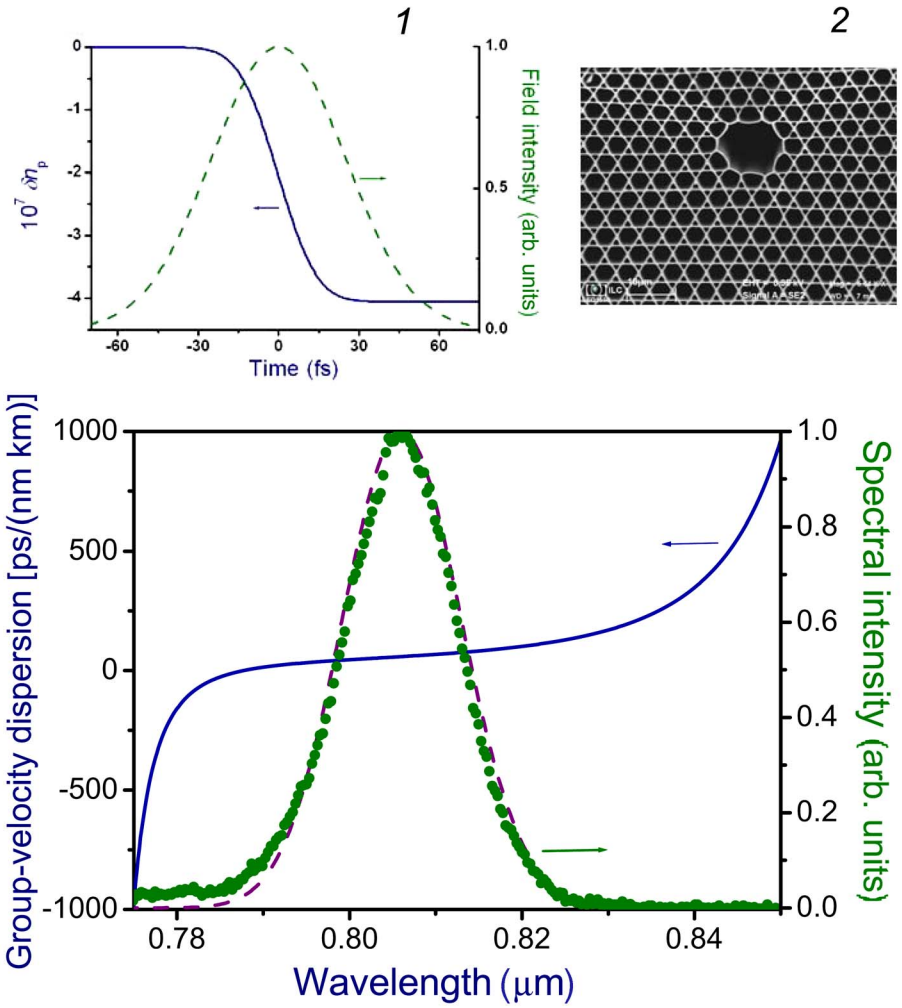

FIG. 1. (Color online) Group-velocity dispersion (solid line) as a function of the wavelength for a hollow-core PCF shown in the inset. Also shown are the spectra of amplified femtosecond Ti: sapphire laser pulses used as a PCF input in experiments (filled circles) and simulations (dashed curve). Inset 1 shows the ionization-induced change in the refractive index δn_p of an atmospheric-pressure air in the field of a laser pulse (shown by the dashed line) with a peak intensity of 5.0×10^{13} W cm^{-2}. Inset 2 presents a scanning electron microscope image of the hollow-core PCF.

field, $R_{\mathrm{core}}(\theta)$ and $R_{\mathrm{cl}}(\theta)$ are the Raman response functions of the gas filling the fiber core and the material of the fiber cladding, $k_0=\omega_0/c$ is the wave number, $\omega_p(z,\tau)=[4\pi e^2 n_e(z,\tau)/m_e]^{1/2}$ is the plasma frequency, e and m_e being the electron charge and mass, respectively.

The nonlinearity coefficients of the core and the cladding are defined as

$$\gamma_{core}=\frac{2\pi}{\lambda}\frac{n_{2g}\int\int_{\Sigma_{core}}|F(x,y)|^4dxdy}{\left[\int\int_{\Sigma_\infty}|F(x,y)|^2dxdy\right]^2}, \tag{2}$$

$$\gamma_{cl}=\frac{2\pi}{\lambda}\frac{n_{2cl}\int\int_{\Sigma_{cl}}|F(x,y)|^4dxdy}{\left[\int\int_{\Sigma_\infty}|F(x,y)|^2dxdy\right]^2}, \tag{3}$$

where n_{2g} and n_{2cl} are the nonlinear refractive indices of the gas filling the fiber core and the material of the fiber cladding, $F(x,y)$ is the transverse field profile in the PCF mode, Σ_{core} and Σ_{cl} are the core and the cladding domains, respectively, Σ_∞ is the infinite domain, and λ is the radiation wavelength. With ionization terms omitted and the nonlinearity of the cladding neglected, Eq. (1) recovers the standard generalized nonlinear Schrödinger equation for pulse dynamics in optical fibers [1].

To include the Raman response of the gas filling the fiber core and the material of the fiber cladding, we solve Eq. (1) with the Raman function of atmospheric air, R_{core}, and the Raman function of silica, R_{cl}:

$$R_{core,cl}(\theta)=(1-f_{1,2})\,\delta(\theta)+f_{1,2}\Theta(\theta)\times\frac{\tau_{1,2}^2+\eta_{1,2}^2}{\tau_{1,2}\eta_{1,2}^2}e^{-\theta/\eta_{1,2}}\sin\left(\frac{\theta}{\tau_{1,2}}\right), \tag{4}$$

where f_i is the fractional contribution of the Raman response, $\delta(\theta)$ and $\Theta(\theta)$ are the delta and the Heaviside step functions, respectively, τ_i and η_i are the characteristic times of the Raman response, and $i=1,2$ for the core and the cladding, respectively. For atmospheric air, $f_1\approx0.5$, $\tau_1\approx62.5$ fs, and $\eta_1\approx77$ fs. For a fused silica PCF cladding, $f_2\approx0.18$, $\tau_2\approx12.5$ fs, and $\eta_2\approx32$ fs.

Ionization effects were included in numerical simulations through the use of the Keldysh model [11] of ionization and the relevant kinetic equation for the electron density [8,9].

We consider a hollow PCF [1,12,13] filled with atmospheric-pressure air with a cross-section structure shown in inset 2 to Fig. 1. Such a waveguide structure provides a high transmission and an anomalous dispersion for a laser pulse with a central wavelength of 807 nm. The wavelength dependence of the group-velocity dispersion (GVD) for this fiber and the input spectrum of the laser pulse are shown, respectively, by the solid and dashed lines in Fig. 1.

Numerical simulations were performed by solving Eq. (1) with the use of the split-step Fourier-transform technique [1]. In these simulations, a 30-ps temporal window was discretized by 2^{17} points. The discretization step Δz for the propagation length was chosen in such a way as to eliminate artifacts originating from numerical instabilities induced by high-order dispersion terms in Eq. (1). With sufficiently small Δz ($\Delta z \approx 10$ μm in our simulations), such instabilities were shifted outside the spectral window, leading to no interference with the spectrum of the laser field within the considered spectral range.

The spectral and temporal evolution of ultrashort laser pulses with a central wavelength of 806 nm in the hollow PCF is presented in Fig. 2. In the regime of low input pulse intensities, femtosecond pulses spread out in time because of the fiber dispersion. This regime of pulse propagation is illustrated in Fig. 2(a), where the input pulse intensity is taken equal to 3.0×10^{12} W/cm^2. The pulse width increases under these conditions from 60 fs at the input of the fiber to approximately 230 fs at the output of a 20-cm PCF section. In this regime, the pulse intensity is too low to induce noticeable ionization of the gas filling the fiber.

In the regime of high input pulse intensities, the dynamics of pulse propagation radically changes. In Figs. 2(b) and 2(c), we illustrate the temporal and spectral evolution of a laser pulse with an input intensity of 5.0×10^{13} W/cm^2. The intensity of such a field is high enough to balance dispersion, giving rise to the formation of solitons. The existence of high-peak-power optical solitons in hollow PCFs has been first demonstrated by Ouzounov *et al.* [14]. As shown by Ivanov *et al.* [15], megawatt-soliton output of hollow PCFs is ideally suited as a source of high-peak-power wavelength tunable radiation for nonlinear microspectroscopy. For longer input pulses, stimulated Raman scattering in gas-filled hollow PCFs has been shown to provide a remarkably high efficiency of frequency conversion [16,17].

At the initial stage of pulse propagation in a hollow PCF considered here [Figs. 2(b) and 2(c)], the soliton dynamics of a laser pulse is manifested as a temporal compression of the laser pulse. A similar solitonic pulse compression of high-peak-power laser pulses in gas-filled hollow PCFs has been earlier reported by Ouzounov *et al.* [18]. An important feature of the dynamics of a high-peak-power light pulse in a hollow PCF considered here is that pulse compression increases the peak intensity of the laser field, enhancing ionization of the gas filling the fiber core. The ionization-induced optical nonlinearity then shifts high-peak-power solitonic features of the laser field toward shorter wavelengths. This shift is clearly seen in the spectral dynamics of the laser field shown in Fig. 2(c). The factors that limit this effect include the loss of energy from the laser field through gas ionization and a limited range of anomalous GVD. Because of these factors, the redshifting of the pulse induced by the Raman effect eventually starts to dominate over the blue shift further on along the fiber.

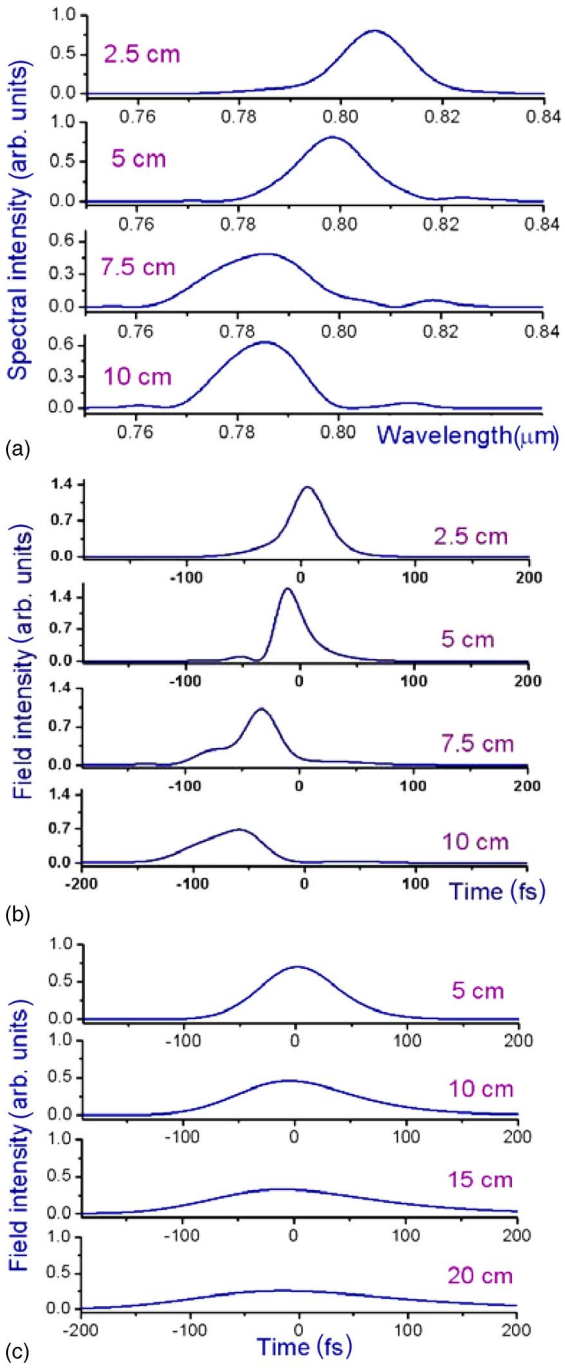

FIG. 2. (Color online) Temporal (a), (b) and spectral (c) dynamics of a laser pulse propagating in a hollow PCF filled with an atmospheric-pressure gas. The input pulse intensity is (a) 3.0×10^{12} W/cm^2 and (b), (c) 5.0×10^{13} W/cm^2. The initial pulse width is 60 fs.

In experiments, we used a hollow-core soft-glass PCF [19] with a core diameter of 13 μm and a period of the photonic-crystal cladding of approximately 5 μm (inset 2 in Fig. 1). The fiber structure is designed to provide a transmission band centered around 800 nm (the dash-dotted line in

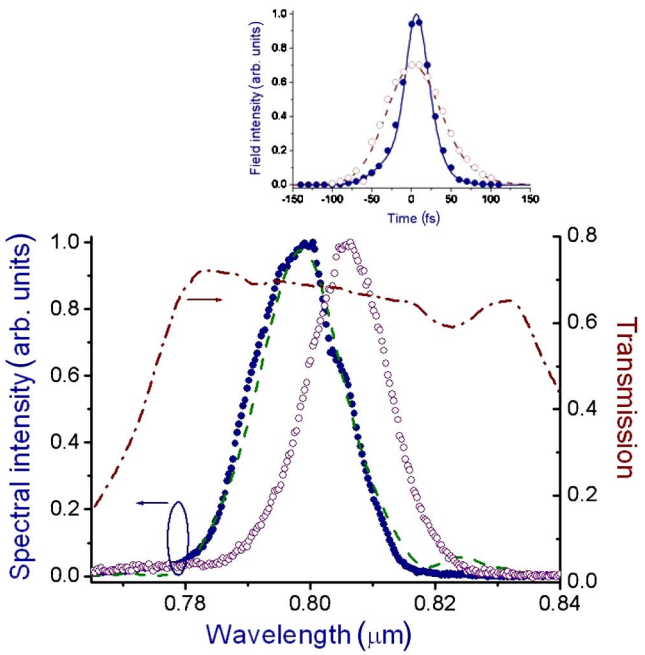

FIG. 3. (Color online) Spectra of amplified Ti: sapphire laser pulses measured at the input (open circles) and at the output (filled circles) of the hollow-core PCF with a length of 5 cm. The initial pulse width is 60 fs. The input pulse intensity is 5×10^{13} W/cm^2. The dashed line shows the results of numerical simulations. Transmission spectrum of the hollow PCF is shown by the dash-dotted line. The inset presents the pulse shape of the PCF output: (solid and dashed lines) results of numerical simulations and (filled and open circles) reconstruction from cross-correlation measurements. The input pulse intensity is (open circles and dashed line) 3.0×10^{12} W/cm^2 and (filled circle and solid line) 5.0×10^{13} W/cm^2.

Fig. 3). The GVD profile for this fiber, calculated using the localized-function technique [20,21], is shown in Fig. 1. Amplified pulses of a mode-locked Ti: sapphire laser with a pulse width of 60 fs and an energy ranging from 50 nJ to 5 μJ are coupled into the hollow core of the fiber with a 6-cm focal length with a coupling efficiency of 80%. The input spectrum of the laser pulses is shown by filled circles in Fig. 1. The effective diameter of the air-guided PCF mode at the output of the fiber was estimated as 10 μm, which agrees well with the results of our numerical analysis of transverse field profiles in the guided modes of the considered type of PCF. Temporal profiles of light pulses transmitted through the PCF were reconstructed in our experiments from the results of cross-correlation measurements. To this end, the PCF output was mixed with a reference 60-fs Ti: sapphire-laser pulse in a 1-mm LBO crystal. The resulting sum-frequency signal was measured as a function of the delay time between the PCF output and the reference pulse.

In the regime of low input laser energies, light pulses tend to spread out in the time domain as they propagate through the PCF in accordance with theoretical predictions presented in Fig. 2(a). Open circles in the inset to Fig. 3 present the pulse shape of the PCF output reconstructed from the cross-correlation trace measured for light pulses with an input energy 140 nJ and an initial pulse width of 60 fs (corresponding to an intensity of 3.0×10^{12} W/cm^2) transmitted through a 5-cm PCF. Experimental results, as can be seen from the inset to Fig. 3, agree well with the results of numerical simulations, shown by the dashed line. The pulse width under these conditions increases from 60 fs at the input of the fiber to approximately 100 fs at the output of the PCF.

For higher input laser intensities, dramatically different scenarios of pulse transformation have been observed. In Fig. 3, we plot the output spectrum of a 5-cm PCF measured for the input pulses with an intensity of 5.0×10^{13} W/cm^2. This intensity was achieved by coupling amplified Ti: sapphire laser pulses with a pulse width of 60 fs and an energy of 2.3 μJ into the hollow core of the fiber. This level of input energies was a factor of 1.5–2.0 below the laser damage threshold of the fiber under our experimental conditions, allowing reliable measurements on the fiber output to be performed. As can be seen from Fig. 3, the spectrum of the PCF output in the regime of high input intensities (filled circles) is noticeably blueshifted with respect to the spectrum of the input pulse (open circles), with the frequency shift estimated as 10 THz. The pulse width of the PCF output under these conditions (filled circles in the inset to Fig. 3) is slightly shorter than the duration of the input pulse, indicating the significance of solitonic effects in spectral and temporal field transformation, as outlined in the discussion above and as illustrated in Figs. 2(b) and 2(c).

The significance of the effects induced by anomalous dispersion of a waveguide structure, including the above-outlined solitonic field transformations, is the key to appreciate the difference between the blueshifting of high-peak-power ultrashort laser pulses in the guided-wave regime and the blueshifting of freely propagating high-intensity ultrashort laser pulses in ionizing gases [7–9]. In the latter case, one either observes blueshifting of intense light pulses within a small focal volume of tightly focused laser beams [7] or deals with a filamentation phenomenon [9,22,23], which provides an efficient spectral transformation of the laser field within larger interaction lengths, but does not offer practical means to control dispersion and the spatial beam dynamics. In the waveguide regime, on the other hand, dispersion can be controlled by designing the waveguide structure, allowing, as shown by our experiments and simulations, temporal spreading of short light pulses to be prevented, while the nature of guided-wave field propagation ensures an excellent quality of the laser beam.

The soliton blueshifting demonstrated by the experiments presented above can only occur within a limited range of laser pulse and waveguide parameters, where the laser fluence is still not detrimental for the waveguide, but ionization is already strong enough to induce spectral shifts exceeding those caused by the Raman effect. Under the conditions of experiments presented here, the soliton compression of the laser pulse, which dominates the dynamics of the laser field at the initial stage of its propagation through the fiber, helps to achieve sufficient field intensities without damaging the waveguide. For the chosen type of hollow PCF, a clearly pronounced reproducible blueshift of the fiber output was observed within the range of input field intensities from 2.0×10^{13} to 9.0×10^{13} W/cm^2. Solitons produced

within the range of input intensities from 8×10^{12} to 1.5×10^{13} W/cm^2 experienced a noticeable redshifting due to the Raman effect. For input intensities above 9.0×10^{13} W/cm^2, a gradual degradation of the fiber transmission, caused by the laser damage of the waveguide, was observed.

We have shown in this paper that the dynamics of ultrashort high-peak-power pulses in gas-filled hollow PCFs may substantially differ from both the free-space evolution of focused-beam intense laser pulses and the standard soliton dynamics observed in waveguides without ionization. While ionization-induced blueshifting is often observed for freely propagating intense ultrashort laser pulses, gas-filled hollow PCFs help to minimize or prevent the temporal spreading of blueshifted high-peak-power laser pulses, allowing a solitonic transmission of such fields. In our experiments, a soliton regime of pulse transmission was demonstrated for ultrashort laser pulses with peak powers of tens of megawatts, providing a high-peak-power blueshifted fiber output with a pulse width less than 60 fs.The interesting features of the demonstrated pulse propagation dynamics relative to standard soliton evolution scenarios are related to the negative change in the refractive index induced by ionization of the gas filling the fiber core. Reversal of the sign of the soliton self-frequency shift is perhaps the most striking consequence of this effect. Experiments presented here demonstrate a 10-THz blueshift of 40-MW laser pulses guided in a hollow-core PCF filled with atmospheric-pressure air. Given the type of a fiber and the sort of gas filling the fiber core, the sign of the frequency shift of the laser field and its rate can thus be controlled by the input laser peak power, offering attractive solutions for the development of high-peak-power wavelength-tunable fiber-format sources of ultrashort pulses, as well as for the processing and regeneration of high-peak power optical signals.

We acknowledge useful discussions with Yu. M. Mikhailova. This study was supported in part by the Russian Foundation for Basic Research (projects 06-02-16880, 07-02-12175, 07-02-91215, and 05-02-90566-NNS), INTAS (projects nos. 03-51-5037 and 03-51-5288),and the U.S. Civilian Research & Development Foundation for the Independent States of the Former Soviet Union (CRDF).

[1] G. P. Agrawal, *Nonlinear Fiber Optics* (Academic, San Diego, 2001).
[2] P. St. J. Russell, Science **299**, 358 (2003).
[3] J. C. Knight, Nature (London) **424**, 847 (2003).
[4] X. Liu, C. Xu, W. H. Knox, J. K. Chandalia, B. J. Eggleton, S. G. Kosinski, and R. S. Windeler, Opt. Lett. **26**, 358 (2001).
[5] D. A. Sidorov-Biryukov, E. E. Serebryannikov, and A. M. Zheltikov, Opt. Lett. **31**, 2323 (2006).
[6] C. Y. Teisset, N. Ishii, T. Fuji, T. Metzger, S. Köhler, R. Holzwarth, A. Baltuska, A. M. Zheltikov, and F. Krausz, Opt. Express **13**, 6550 (2005).
[7] W. M. Wood, C. W. Siders, and M. C. Downer, Phys. Rev. Lett. **67**, 3523 (1991).
[8] V. P. Kandidov, O. G. Kosareva, I. S. Golubtsov, W. Liu, A. Becker, N. Akozbek, C. M. Bowden, and S. L. Chin, Appl. Phys. B: Lasers Opt. **77**, 149 (2003).
[9] P. Sprangle, J. R. Penano, and B. Hafizi, Phys. Rev. E **66**, 046418 (2002).
[10] E. E. Serebryannikov and A. M. Zheltikov, Phys. Rev. A **76**, 013820 (2007).
[11] L. V. Keldysh, Sov. Phys. JETP **20**, 1307 (1965).
[12] R. F. Cregan, B. J. Mangan, J. C. Knight, T. A. Birks, P. St. J. Russell, P. J. Roberts, and D. A. Allan, Science **285**, 1537 (1999).
[13] C. M. Smith, N. Venkataraman, M. T. Gallagher, D. Muller, J. A. West, N. F. Borrelli, D. C. Allan, and K. W. Koch, Nature (London) **424**, 657 (2003).
[14] D. G. Ouzounov, F. R. Ahmad, D. Muller, N. Venkataraman, M. T. Gallagher, M. G. Thomas, J. Silcox, K. W. Koch, and A. L. Gaeta, Science **301**, 1702 (2003).
[15] A. A. Ivanov, A. A. Podshivalov, and A. M. Zheltikov, Opt. Lett. **31**, 3318 (2006).
[16] F. Benabid, J. C. Knight, G. Antonopoulos, and P. St. J. Russell, Science **298**, 399 (2002).
[17] F. Benabid, G. Bouwmans, J. C. Knight, P. St. J. Russell, and F. Couny, Phys. Rev. Lett. **93**, 123903 (2004).
[18] D. Ouzounov, C. Hensley, A. Gaeta, N. Venkateraman, M. Gallagher, and K. Koch, Opt. Express **13**, 6153 (2005).
[19] S. O. Konorov, A. B. Fedotov, O. A. Kolevatova, V. I. Beloglazov, N. B. Skibina, A. V. Shcherbakov, and A. M. Zheltikov, JETP Lett. **76**, 341 (2002).
[20] L. Poladian, N. A. Issa, and T. M. Monro, Opt. Express **10**, 449 (2002).
[21] S. O. Konorov, E. E. Serebryannikov, A. B. Fedotov, R. B. Miles, and A. M. Zheltikov, Phys. Rev. E **71**, 057603 (2005).
[22] A. Braun, G. Korn, X. Liu, D. Du, J. Squier, and G. Mourou, Opt. Lett. **20**, 73 (1995).
[23] J. Kasparian, M. Rodriguez, G. Mejean, J. Yu, E. Salmon, H. Wille, R. Bourayou, S. Frey, Y. B. Andre, A. Mysyrowicz, R. Sauerbrey, J. P. Wolf, and L. Woeste, Science **301**, 61 (2003).